Final Report

For

Hybrid Active-Passive Systems for Control of Aircraft Interior Noise

Prof. Chris R. Fuller, PI

Contract Period: 1/1/99-3/31/02

Virginia Polytechnic Institute and State University
Vibration and Acoustics Laboratories
Department of Mechanical Engineering
131 Durham Hall
Virginia Polytechnic Institute and State University
Blacksburg, VA 24061-0238

Grant Number: NAG-1-2158

PROPOSED RESEARCH

It was proposed to continue with development and application in the two active-passive areas of Active Tuned Vibration Absorbers (ATVA) and smart foam applied to the reduction of interior noise in aircraft. In general the work was focused on making both techniques more efficient, practical and robust thus increasing their application potential. The work was also concerned with demonstrating the potential of these two technologies under realistic implementations as well as understanding the fundamental physics of the systems.

The proposed work consisted of a three-year program and was tightly coordinated with related work being carried out in the Structural Acoustics Branch at NASA LaRC. The work was supervised and coordinated through all phases by Prof. Chris Fuller of Va Tech.

WORK PERFORMED

Since a summary of the first two years of the project has been presented to NASA via progress reports and presentations at NASA Interior Noise workshop, this report will mainly focus on work of the last year of the project. However it should be noted that the work of the last year relies and builds upon the work performed in the first two years.

Two main research topics were investigated;

A. Use of advanced ATVA's for interior noise reduction

A1. Motivation

The ATVA project is motivated as a potential solution to the interior noise problem in propeller aircraft. The tonal nature of the blade passing frequency (BPF) disturbance has inspired researchers to treat the fuselage with TVA's tuned precisely to the BPF in an attempt to significantly increase the structural impedance at this frequency, thus achieving better rejection of the propeller induced acoustic disturbance. To date, this approach has demonstrated limited success in reducing interior sound levels and proven to be sensitive to changes in the disturbance frequency during flight.

Previous research, Maillard & Fuller '95, (Ref. 1) has suggested that TVA's could control interior noise by restructuring the vibrational energy in the fuselage from modes that couple well to the interior sound field to more poorly coupled structural modes. This is achieved by allowing the resonant frequency to deviate from the excitation frequency, resulting in a mechanical input impedance (that is added to the structure by the TVA's) that appears mass-like or stiffness-like. Termed *global detuning*, this approach uses a

minimization algorithm to monitor a global cost quantity such as radiated acoustic energy and direct the detuning of the TVA's. In practice, this noise control scheme requires TVA's with the ability to change their resonant frequencies. The ATVA project addresses the development of such devices as well as proof-of-concept experimental work that demonstrates significant reduction of structural radiated noise using ATVA's.

A2. Project Goals

There are two major goals to the ATVA project:

1. Develop an ATVA suitable for use as a component of a noise control system.
2. Demonstrate, experimentally, the ability of an ATVA noise control system to reduce structurally radiated sound.

To accomplish Goal #1, a method is developed to control the input impedance of an inertial actuator. A feedback loop is introduced to the inertial actuator which measures the motion of the actuator mass and produces a control signal to drive the active force element. The result is an ATVA whose resonant frequency and Q factor can be controlled *independently* through a wide range of tuning configurations.

To accomplish Goal #2, a control algorithm is employed to adapt the resonant frequency and damping of a set of ATVA's applied to a structure while monitoring a global acoustic cost quantity to be minimized. A geometrically inspired search algorithm is chosen which requires no initial information about the structure or the ATVA's. The global control algorithm monitors several microphones by interfacing with a data acquisition system and controls the ATVA's via DC voltage outputs that determine the feedback control gains.

Together, these two goals comprise a hierarchal noise control scheme. The global tier is the control algorithm that monitors the global cost quantity and directs the adaptation of the ATVA's by changing the feedback control gains. The subordinate (local) tier consists of the ATVA's, comprised of the inertial actuators and their local feedback loops. The ATVA's are all independent and do not exchange information with one another or with the global controller. Each ATVA requires only local information (i.e. the motion of its own mass) as well as the feedback control gains determined by the global controller.

A3. ATVA Development

The inertial actuators are initially modeled as single-degree-of-freedom (SDOF) systems with an active force in parallel with the spring and damper. Then, a feedback loop is introduced from the absolute motion of the mass to the active force input (Figure 1). Feeding the absolute mass velocity back through a purely real gain results in an equivalent passive system that contains a "skyhook" damper. Using absolute displacement feedback would result in a "skyhook" spring.

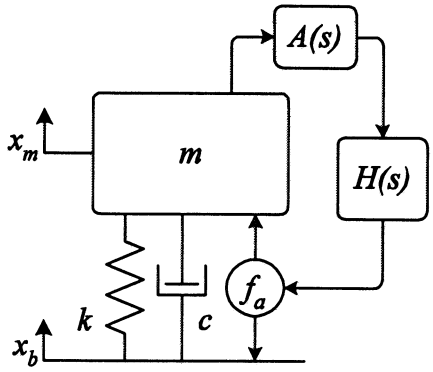

Figure 1. Feedback loop from the absolute motion of the mass to the active force input.

Analog *PI* feedback (Eq. 1) is chosen to control the ATVA's. Analog *PI* control is chosen for several reasons. First, it produces a control signal whose two components are related by a time derivative, just like the forces of a spring and damper. Second, it allows for each component of the control signal applied *simultaneously*, yet be determined *independently* as they are truly orthogonal to one another. Third, a low cost analog circuit can be readily built to act as the feedback controller.

Velocity is chosen as the feedback signal (Eq. 2), so *PI* feedback control simultaneously applies a "skyhook" damper and spring to the inertial actuator to independently adapt the closed loop stiffness and damping of the ATVA. The closed loop characteristic equation for the ATVA is Equation 3.

$$H(s) = K_p + \frac{K_i}{s} \qquad \text{Equation (1)}$$

$$A(s) = s \qquad \text{Equation (2)}$$

$$ms^2 + (c - K_p)s + (k - K_i) = 0 \qquad \text{Equation (3)}$$

From the characteristic equation, it is seen that K_p behaves like "active damping" and K_i behaves like "active stiffness" when velocity feedback is used. Figure 2 is the equivalent "passive" system for the ATVA using mass velocity feedback with analog *PI* control.

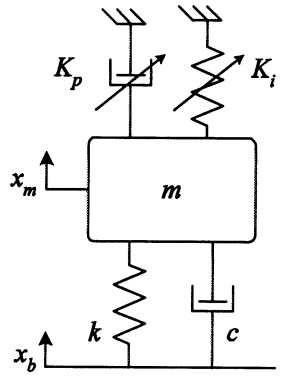

Figure 2. The equivalent "passive" system for the ATVA using mass velocity feedback with analog *PI* control.

Analog Control Circuit

An accelerometer measures the motion of the mass, so the signal must first be integrated to obtain velocity. An analog control circuit was designed and built to accomplish this as well as to apply the feedback control gains and construct the control signal from the two components. Figure 3 is a schematic of the signal flow through the *PI* control circuit. Feedback control gains are set in the control circuit by externally applied DC voltages by which the control signal components are multiplied. Under this method of applying control gains, 1 V_{DC} equals a control gain of 1.

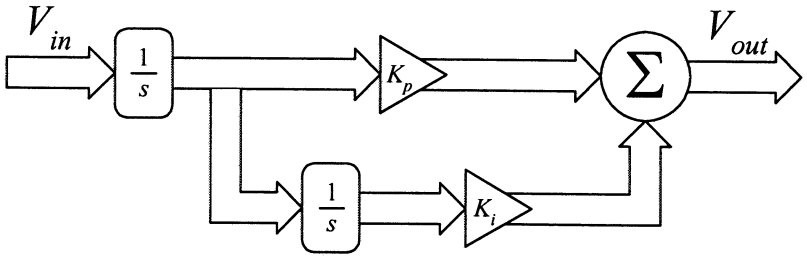

Figure 3. Schematic of the signal flow through the *PI* control circuit.

A model was also built of the analog control circuit and used to design and predict the response. Figure 4 shows the agreement between the measured and predicted responses for K_p =1. Figure 5 is the same for K_i =1 and the two curves deviate only at very low frequency where there is poor coherence from insufficient excitation energy. Overall there is excellent agreement between the measured and predicted response of the control circuit.

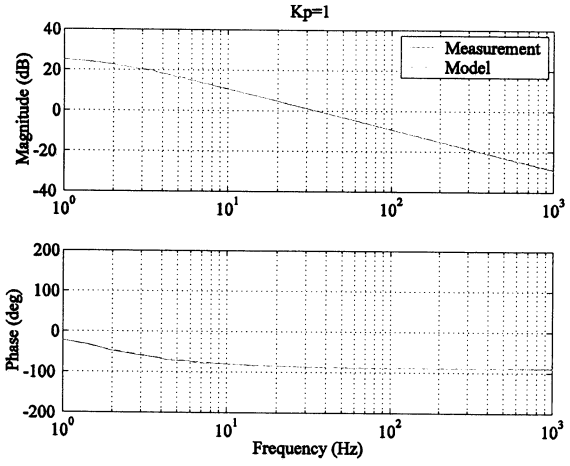

Figure 4. Measured and predicted responses for K_p =1, K_i =0.

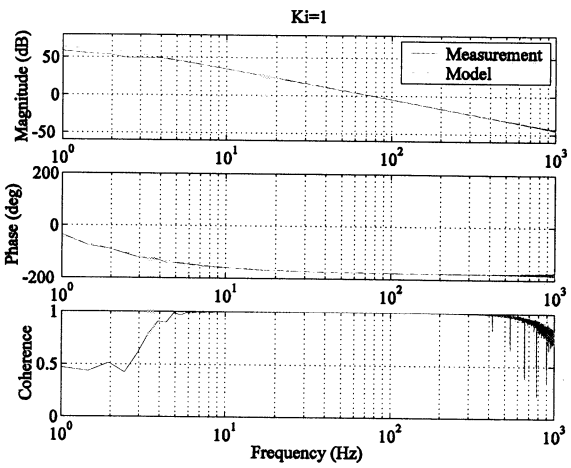

Figure 5. Measured and predicted responses for K_i =1, K_p =0.

ATVA Tuning

A detailed analytical model was built of the Motran inertial actuator that includes the transduction dynamics of the voice coil element and the dynamics of the feedback control circuit and power amplifier. This model was used to predict the closed loop transmissibility of the ATVA for both stiffness tuning and damping control. It is also used to study the stability limitations of the ATVA.

A Motran ATVA is pictured in Figure 6 mounted on a 50 lb. shaker, used for excitation, and instrumented with accelerometers and a force gauge for transmissibility measurements. Figure 7 presents a comparison of the predicted and measured transmissibilities for a set of control gains that spans the entire stable tuning range of the ATVA. The measured transmissibilities are plotted in black and the modeled curves are generated using only the spectral line frequencies from the measurements for better comparison.

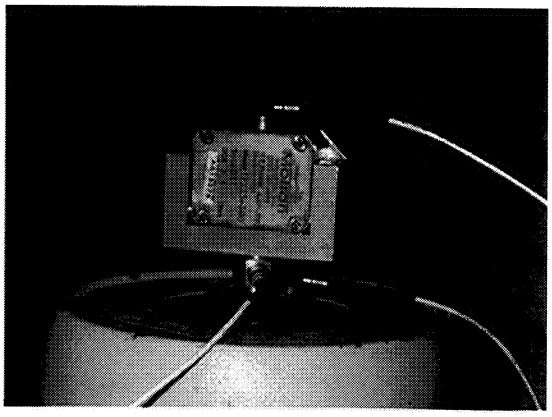

Figure 6. ATVA instrumented for transmissibility measurements.

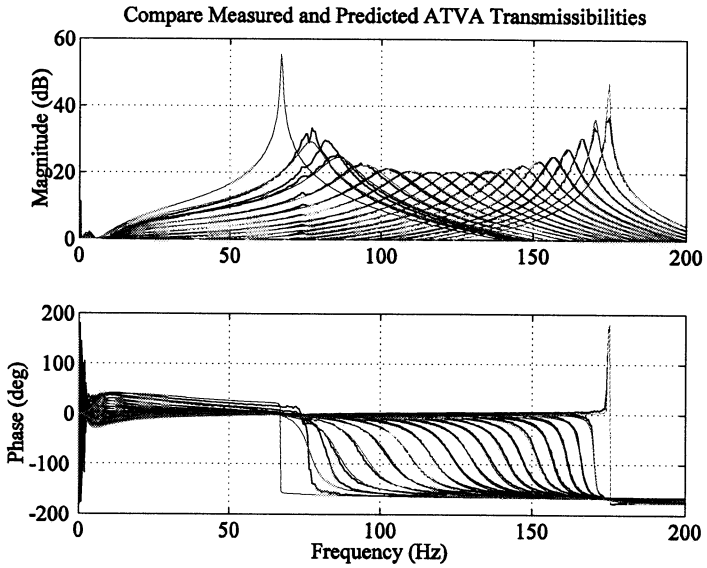

Figure 7. Predicted and measured ATVA stiffness tuning transmissibilities.

The stable closed loop tuning frequency range is about 75-175 Hz or about ± 40% of the passive natural frequency of the ATVA, which is about 124 Hz. There is excellent agreement between the two sets of curves indicating that the ATVA is indeed well understood. The model captures the low frequency phase behavior seen in the measurements. The primary deviation between the two sets of curves is at low frequency where the predicted resonant frequencies are lower than those measured. Figure 8 is a root locus plot generated with the ATVA model that explains the nature of the stability limits as well as the fact damping disappears from the ATVA towards these limits. The low frequency poles are all contributed by the control hardware and cause the resonant poles to cross the imaginary axis at both the upper and lower frequency stability limit.

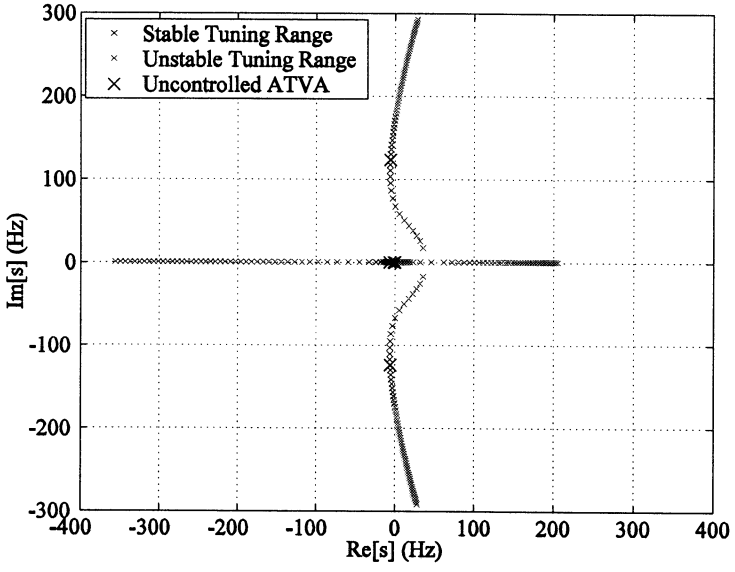

Figure 8. Root locus for ATVA stiffness tuning.

The ATVA has been observed to have the ability to remain stable for small gain margins beyond the gain at which the resonant poles are marginally stable. This result is non-intuitive and is attributed to two things. First, a small stable gain margin is predicted by theory as a result of using absolute velocity feedback rather than the relative velocity between the mass and the base. Second, some energy dissipation occurs in the excitation shaker, which can prevent a slightly unstable ATVA from destabilizing the coupled system.

ATVA Damping Control

Damping control experiments were also performed and Figure 9 presents the measured set of transmissibilities plotted against those predicted by the model. Again, excellent agreement between the data sets is observed. The ATVA can be adapted to have a damping value ranging from about zero where the device is marginally stable to a very large value at which the device does not appear resonant.

A root locus of the damping control, generated by the model, is included in Figure 10. This root locus demonstrates that the damping control gain behaves very much like natural damping.

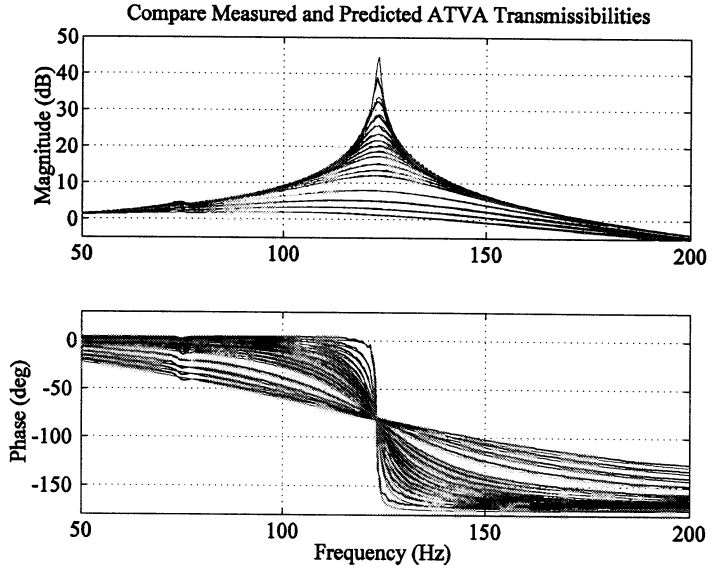

Figure 9. Predicted and measured ATVA damping control transmissibilities.

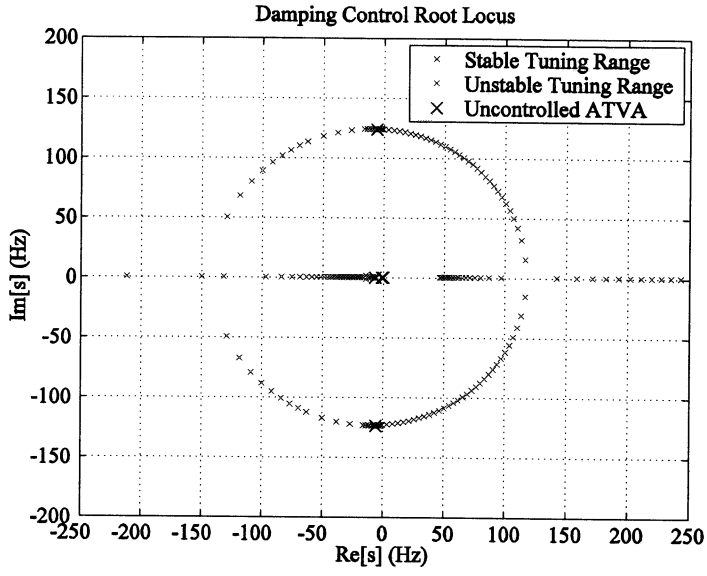

Figure 10. Root locus for ATVA damping control.

A4. ATVA Noise Control

The ATVA noise control system requires a central minimization algorithm to monitor a global cost quantity and direct the ATVA's detuning via the feedback control gains. The average of several squared microphone pressures is used as an estimate of the radiated acoustic energy, which is chosen as the global cost. Accelerometers are mounted to the structure at the base and mass of each ATVA. The mass accelerometer signals are required as the input to the local feedback control loops. These signals are also used in conjunction with the base accelerometer signals to evaluate the ATVA's transmissibilities, particularly the relative phase. The base accelerometers allow changes in base vibration levels to be observed throughout the experimental work. The base accelerometers, however, are not required to implement the ATVA's.

The entire ATVA noise control system resides in a single PC. Dynamic microphone and accelerometer are acquired by a PC data acquisition (DAQ) card from National Instruments (NI) that is interfaced by custom software written in LabVIEW. The DC voltages that become the feedback control gains are generated by a separate NI analog output card in the PC that is also interfaced using custom software written in LabVIEW. Accordingly, all of the control code was written in LabVIEW to result in a single platform, stand alone noise control system.

Typical Cost Function Surface

The cost function surface has been mapped experimentally using a simply supported plate test structure and a single ATVA. The cost function was also evaluated analytically using a model of the test plate with a TVA present. The results are very similar and a typical cost function surface produced by the model is shown in Figure 11 for an excitation frequency of 100 Hz.

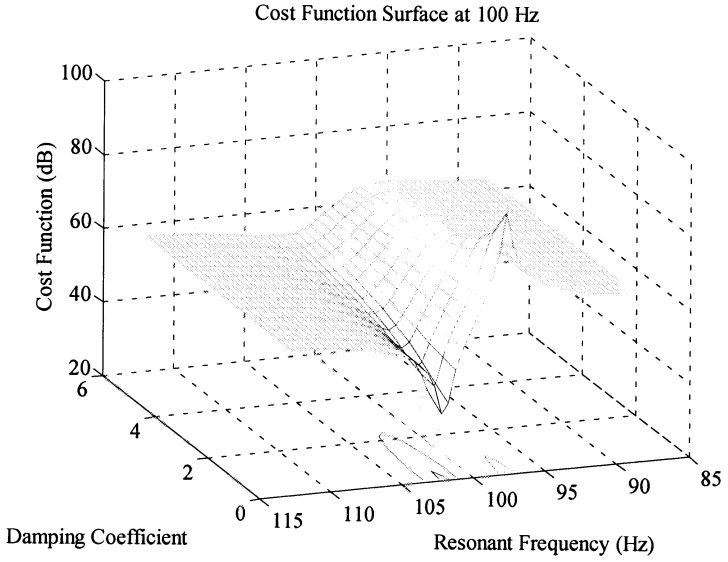

Figure 11. Cost function surface for a simply supported plate with a single ATVA.

The surface is smooth, consisting of only a single minimum and maximum, which are traversed as the stiffness tuning gain (resonant frequency) is changed. There are no local minimums to trap a search algorithm. The ATVA has the most profound effect on the cost function when its damping is minimized and its effect is diminished as damping is added. The effect of the ATVA is also found to decrease as it is tuned far away from the excitation frequency. This happens because the input impedance of a TVA becomes negligible at frequencies far away from resonance.

The maximum and minimum values are always observed to be separated by the condition when the ATVA is perfectly tuned to the excitation frequency (i.e. stiffness control gain that perfectly tunes the ATVA to -90° phase). A theoretical basis for this observational consistency has not yet been firmly established.

The proposed detuning method is to first tune the ATVA's to the excitation frequency using the phase between the base and mass accelerometer signals. Based on consistent observations, tuning the ATVA's first will locate the initial control gains on the correct side of the cost surface maximum value so the minimum can be found by the downhill search. Once tuned, the downhill simplex detuning algorithm is started.

Global Minimization Algorithm

The minimization algorithm chosen to direct the detuning of the ATVA's is called the Downhill Simplex Search. This algorithm requires no initial information about the structure or ATVA's and simply follows a set of rules to guide the search "downhill." The algorithm is geometrically inspired and works by creating the simplest possible geometric shape (a simplex) in the space spanned by the control parameters.

The ATVA's are detuned sequentially so there are two control parameters, the feedback control gains K_p and K_i. The simplest geometric shape in 2-space is a triangle. In this case, the three vertices of the simplex are evaluated and a new trial point is generated by reflecting the worst (highest) vertex about the centroid of the simplex. The cost at this point is then compared to the three original points and its relative value determines the next algorithm step. By reflecting, expanding, contracting, and constantly replacing worse vertex points with better ones, the algorithm "walks" downhill towards the minimum value. This algorithm is covered in detail by Nelder and Mead (Ref 2).

Preliminary Noise Control Results

As an initial test structure, a large steel plate (6'x 4'x 3/32") was "baffled" by enclosing it in a 6" deep wooden enclosure. The plate is supported under its own weight on a bead of silicon that was applied around the rim of the enclosure and allowed to cure before the plate was placed on top. This creates an unknown boundary condition between free and simply supported.

A large plate was chosen because it is a relatively simple structure that is modally dense near the passive resonance of the ATVA, but not completely understood due to the unknown boundary conditions. The passive resonance of the ATVA is approximately the center of the stable tuning frequency range. A modally dense structure near this passive resonance is required if noise control is to be achieved by "modal restructuring."

Only preliminary noise control results have been obtained at this time. Inside an anechoic chamber, the structure was excited at 120 Hz by another Motran inertial actuator with a passive resonance of about an 88 Hz. Five ATVA's were placed randomly on the plate, perfectly tuned to -90° phase, and then sequentially detuned using the downhill simplex algorithm. A single microphone located about 8 feet above the plate was used to measure the global cost. The feedback control gains were constrained to ensure system stability. The ATVA's were sequentially detuned for five complete iterations, each iteration beginning at the previous end condition. Table 1 summarizes the experimental global detuning results using multiple ATVA's.

Large Plate test rig – 5 ATVA's - 120 Hz Tonal Excitation		
Uncontrolled	Perfectly Tuned	Globally Detuned
0 dB (baseline)	-1 dB	-20 dB

Table 1. Experimental global detuning results using multiple ATVA's.

Interestingly, 3 of the 5 ATVA's reached the imposed feedback gain constraints during the global detuning. This result implies that the optimal impedance at those locations is not large, but rather mass-like for those that reached the lower tuning limit and stiffness-like for those that reached the upper tuning limit. This result is consistent with the analytical results obtained by Maillard and Fuller that motivated this ATVA project.

For this test case, perfectly tuning all ATVA's has little effect on the radiated sound at the error microphone. This implies that either the ATVA's do not have enough authority to reduce the structural vibration at this frequency, or that the structure has more than five degrees-of-freedom (modes) participating at this excitation frequency. Inspection of the base accelerometer signal reveals that the base vibration is reduced significantly when the ATVA's are tuned, so the first conclusion is that the ATVA's authority is sufficient. But, since pinning the plate at the five attachment points does little to reduce the sound radiation, the second conclusion is that enough modes are indeed participating to still allow sound radiation at this excitation frequency. The question of why the ATVA's distributed impedance does little to reduce the cost function when tuned, but has a profound effect when detuned is left to be answered.

A5. Conclusions

An ATVA has been developed using analog *PI* feedback control. The resonant frequency and Q factor can be controlled independently via the orthogonal feedback control gains. An experimental stable tuning range of about 75-175 Hz is demonstrated, which is about ±40% around the passive resonance frequency (124 Hz). A stable damping range from marginally stable to highly damped has also been experimentally demonstrated. Enough damping can be added to the ATVA so that it does not even appear to be a resonant system.

An analytical model of the Motran ATVA has been developed and validated by predicting the measured behavior of the ATVA very accurately. This model requires the inclusion of all the dynamics in the control circuit, the power amplifier, the transduction dynamics of the voice coil, as well as the mechanical parameters of the inertial actuator. Stability of the ATVA has been studied and the nature of the instabilities identified. This information may be used in the future to develop ATVA's with larger stable tuning ranges.

An analog circuit has been designed to implement the *PI* feedback control scheme and experimentally validated. The analog circuit was analytically modeled and its predicted responses match measurements to a high degree of accuracy. More importantly, the control circuit has demonstrated the ability to adapt the closed loop resonant properties of the ATVA for which it was designed.

The radiated sound cost function surface has been identified for a plate structure both experimentally and predicted analytically, with agreement. The cost function is smooth with a single (global) maximum and minimum. A suitable global detuning search algorithm has been identified as the downhill simplex search and implemented in LabVIEW. A method has been proposed to first tune the ATVA's to -90° phase to ensure a favorable initial location, and then start the global detuning algorithm.

A compact, robust ATVA noise control system has been developed on a single platform (LabVIEW), Windows-based PC. The DAQ system, the DC output voltage (control gain) hardware is interfaced through software that is embedded into the ATVA control

algorithm software. The result is a software interfaced, stand alone ATVA noise control system.

Preliminary detuning experimental results from a modally dense plate with unknown boundary conditions have been obtained for a 120 Hz tonal excitation. It is found that detuning five ATVA's placed randomly results in 20 dB reduction of sound radiation, outperforming perfectly tuned ATVA's which yielded virtually no sound reduction over the uncontrolled case. Three out of five ATVA's reached stability imposed tuning limits, implying that smaller mass-like and stiffness-like reactive impedances are required to achieve noise control at several ATVA locations. This result is in contrast to the conventional TVA noise control approach, which seeks to stop structural vibration at the excitation frequency using the very large impedances of many perfectly tuned devices.

Other work was concerned with applying the ATVA's to laboratory fuselage structures and also to a flight test on a Cessna 182. While the laboratory fuselage tests showed good reductions of the de-tuned ATVA system the flight tests did not provide good performance. This was thought to be due to two main reasons; firstly the tuning algorithm was not fully developed at that stage of the work. Secondly the positioning of the ATVA's on regions of reasonable mobility was not properly optimized due to lack of testing time. Now that a good tuning approach and hardware has been developed further flight-testing is needed. Full details of the ATVA work will be available in a Doctoral Thesis based upon the project.

A6. Future Work

Work remains to find experimental evidence to explain how noise control is achieved by detuning several ATVA's attached to a structure. The large plate test rig will be used initially to answer this question. The plate will be scanned with accelerometers to measure the structural response in the uncontrolled, tuned, and detuned configurations. A two-dimensional wavenumber transform will be used to evaluate the radiation efficiency of the plate for each ATVA configuration.

The expected result is that energy will move from wavenumbers inside the radiating region to outside wavenumbers when the ATVA's are detuned from the initial tuning. Work also remains to find a theoretical explanation as to why the global cost maximum and minimum seem to always be separated by the perfectly tuned ATVA.

B. Control of boundary layer interior noise using smart foam

B1. Goals

The main goals of this research effort were to (i) improve the low frequency performance of the smart foam treatment (ii) develop realistic smart foam configurations and demonstrate their potential in wind tunnel tests and (iii) develop and test less complex arrangements of smart foam treatment and also demonstrate that satisfactory performance

is still achieved. Goal (i) was approached by integrating knowledge from related work on DVA's and DAVA's into the smart foam. It was planned to achieve goal (ii) by integrating the sensors into or near the smart foam elements. The smart foam system would attenuate turbulent boundary layer induced interior noise in aircraft by minimizing mean square pressure in the near field thus unloading the structure. Efforts for goal (iii) were also conducted to explore the trade-offs of using decoupled control strategies. In addition, several means of reference and error sensing methods were explored for their abilities to increase control performance. This was to be done while also reducing computational overhead of the control system.

B2. Work of first two years

Figure 12 shows the wind tunnel and anechoic box system used for the smart foam tests at VAL, Va Tech. Figure 13 shows an array of six smart foam actuators located on an aircraft panel in related wind tunnel tests at NASA LaRC. Figure 14 shows a schematic of the general test system and control arrangement. Turbulent boundary layer flow is used to excite a thin aircraft like panel located in the wall of the wind tunnel. Smart foam elements are located on the panel and used in an active-passive approach to reduce the boundary noise transmitted through the panel into the anechoic enclosure. An array of microphones is used in the enclosure to monitor the transmitted boundary layer noise. A digital adaptive Filtered X feedforward control approach is used. Reference sensors are located under each smart foam element while selected microphones form the anechoic box array are used as errors sensors.

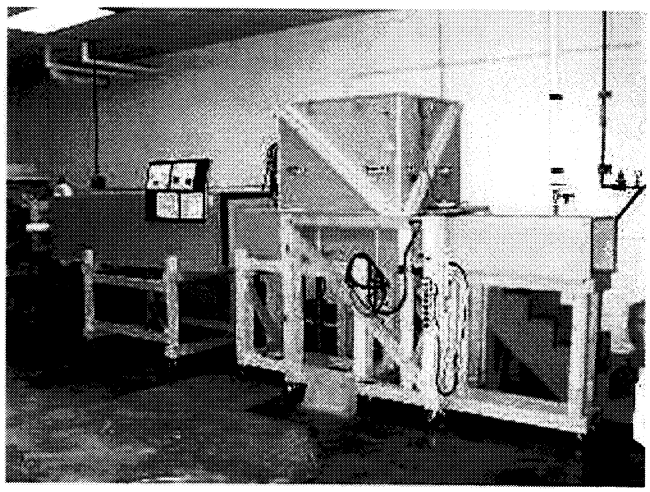

Figure 12. Smart foam wind tunnel test rig at VAL, Va Tech.

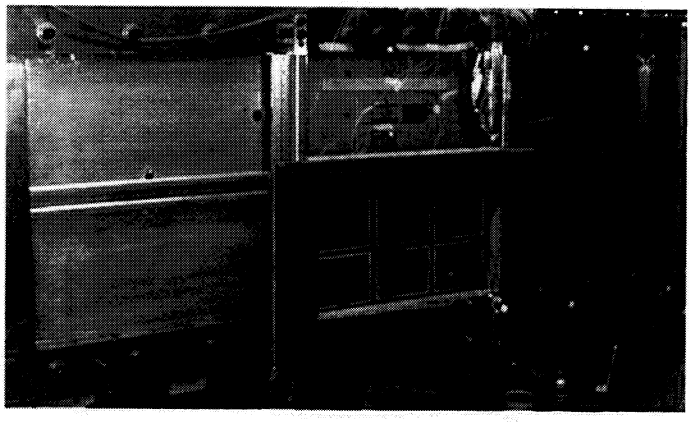

Figure 13. Smart foam actuators located on NASA LaRC aircraft panel.

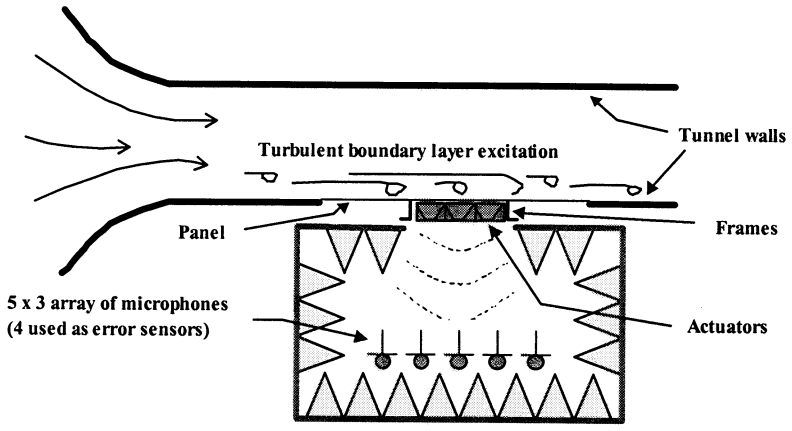

Figure 14. Schematic of test rig and smart foam treatment.

Figure 15 shows a typical early performance curve achieved with a four-reference sensor under the six smart foam actuators. Two pairs of smart foam actuators were wired together to create a single channel of control. Four microphones were used as error sensors. The digital control system was thus 4 by 4 by 4 with a design control bandwidth of 400 to 1000Hz. The flow speed was set at M=0.12. Very good passive and reasonable active-passive attenuation is observed in the control bandwidth. Poor active attenuation is observed at the low frequency peak of 210Hz due to the lack of control output from the smart foam actuators at very low frequencies.

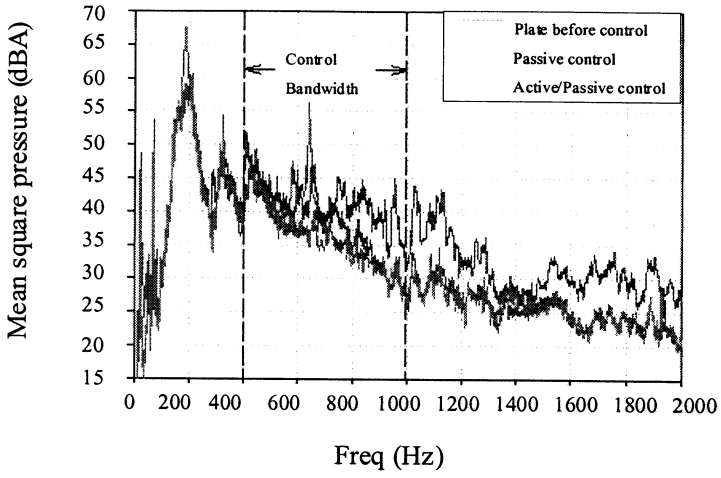

Figure 15. Performance of early smart foam treatment.

Although this early work showed good performance of the smart foam treatment there were several issues that need improvement. Firstly, the reference and error microphones needed integration into the smart foam system if possible in order to create a compact and practical treatment. Secondly, the low frequency actuation limitation of the smart foam elements needed to be improved. Thirdly, the performance of the smart foam is limited by the multiple coherence between the reference sensors and error microphones. Adding more reference sensors is likely to increase the multiple coherence and thus the control performance. However implementing more reference sensors markedly increases the DSP CPU requirement to the point it impacts the control performance via reduced sampling rate and filter lengths. Thus less complex control configurations are needed in order to alleviate this negative effect and this was a fourth issue to be studied in the project.

Work on the project in the first year was concerned with improving the low frequency output of the smart foam actuators. This was achieved by locating a thin metal plate over the top of each smart foam element. This distributed mass acted with the foam structure to create a dynamic resonant system. Thus the output of the smart foam element could be increased at chosen resonant frequencies or the element could be used to reactively attenuate vibration of the panel on which it was located. Wind tunnel tests using the system described next demonstrated that such a system significantly improved the low frequency attenuation without reducing the high frequency performance. The dominant tone present in the noise spectra around 210Hz and associated with the fundamental resonance of the plate was well attenuated. This work has been reported in detail at a number of NASA interior noise workshops.

B3. Work of the last year

More recent work was concerned with goals (ii) and (iii). For goal (ii) the procedure used involved the use of a lightweight active skin treatment applied to the interior surface of a representative fuselage panel subjected to a subsonic turbulent flow. The active skin

treatment consisted of several smart foam actuators along with reference sensors mounted to the vibrating panel and error sensors located in the acoustic near field. Smart foam was chosen, as opposed to ordinary loud speakers, primarily for their lightweight as required in aircraft noise control applications. In addition, their foam construction allowed for passive attenuation at higher frequencies by means of absorption and their geometry could be tailored allowing various control schemes to be explored. Early work using far field error sensors in conjunction with a MIMO digital feedforward controller had demonstrated the good potential of such a system. This work has been reported in detail at NASA interior noise workshops. However the practicality of the smart foam treatment would be improved if all the transducers were integrated into its structure. This work is now briefly summarized. Full details will be available in a Doctoral Thesis based upon the project work.

Error sensors were designed to reject near field acoustics as well as to be directional such that the majority of the error sensor response would be due to the smart foam actuator and noise radiating from the vicinity of the panel closest to it. Error sensors used were microphone arrays consisting of three summed microphones equally spaced on a ring. The diameter of the ring was chosen based on maximum directivity achieved at the upper frequency of the control band of interest, 400—800 Hz. An analytical procedure for investigating the array performance and optimizing its configuration was developed. The resulting array of three microphones was chosen to have a radius of 38 mm.

Reference arrays were also designed to increase coherence between measured panel vibration and the interior noise field. Although various methods were explored for reference sensing, including the use of PVDF spatial filters, the technique proving most successful for active control involved the use of multiple, independent point reference measurements per actuator. Sensors used were ordinary accelerometers mounted to the radiating panel. For each actuator, three accelerometers were mounted in a circle having a radius of 15 mm. The circular arrangement was collocated with the center of the respective actuator.

A time domain model of the open loop and controlled dynamic system was developed. This model was based upon constructing time domain digital filters from measured system transfer functions. The full adaptive time domain LMS paradigm was also simulated. Predicted performance of different system configurations could thus be obtained from pre-measured system data.

Multiple coherence studies between a single microphone centered 100 mm above a 50 mm grid of fourteen accelerometers were performed with theoretically maximum achievable control (calculated using the simulation above) plotted in Figure 16. By the figure, it is shown that increasing the number of accelerometers increases the multiple coherence, however diminishing returns occur when using more than four.

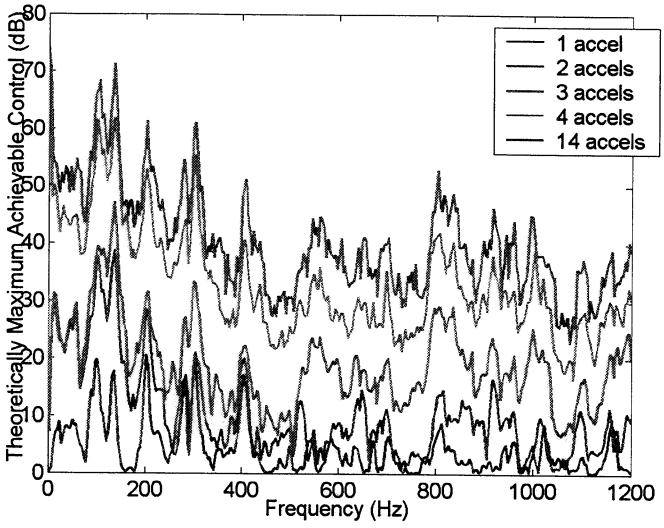

Figure 16. Theoretically maximum achievable control.

We now discuss results associated with goal (iii). This area was concerned with studying various coupled and uncoupled control arrangements in order to reduce the system complexity and computational overhead. Four-channel control was performed by experiment and eight-channel control was performed using control simulations (see model developed above) based on experimentally determined data due to CPU limitation on the DSP. The control simulation software was quantified to within 0.1 dB_A by comparing identical control simulations and experiments for the four-channel case. The laboratory wind tunnel test rig was identical to that summarized in previous progress and workshop reports and shown in Figure 12. A simulated aircraft panel was located in the side of a Va Tech wind tunnel and driven by boundary flow of up to M=0.12. The radiated sound field from the panel was measured by an array of twelve microphones located in an anechoic chamber surrounding the panel. Much work was carried out to isolate the interior field from acoustic and structural flanking paths using the anechoic box shown in Figure 12 and also to quantify the boundary layer interior noise. Extensive work was done to design and install a duct muffler to quiet the fan noise shown in Figure 12. Eight smart foam elements were located on the test panel. All control except the uncoupled 8 by 8 approach were implemented on a TI C40 Quad 4 DSP system.

The control configurations studied consisted of; (i) fully coupled MIMO control with various number of reference sensors under each smart foam element and (ii) multiple uncoupled SISO loops with various number of reference sensors. Performance of active minimization of mean square sound pressure (summed over the microphone array) using smart foam was successfully achieved at the error sensors. Far field control was achieved using multi-channel control utilizing far field error sensors. The results show that fully coupled MIMO or multiple uncoupled single channel SISO (mSISO), control may be implemented with success. Four channels of 4I4O control over a 400-800 Hz band resulted in 3.2 dB_A attenuation for MIMO and 2.3 dB_A for mSISO. Although four channel performance using mSISO control was 1 dB_A less than for the MIMO case, the

number of computations required was significantly less and therefore may be considered an acceptable trade-off. For the four-channel configuration used, MIMO would require a factor of 256 more computations to determine the control filters than would mSISO.

We now study the performance of the near field, integrated sensor arrays. Control was performed with error arrays located 10 cm above the smart foam elements and performance at observer microphones, mounted 40 cm above the error arrays, and were monitored. Multiple, point-measured references per actuator were used. MIMO and multiple MISO[1] (mMISO) control utilized one, two, or three reference accelerometers mounted on a 15 mm radius as previously discussed. Example results for the summed power of the error sensors are presented in Figure 17.

Comparing eight channel MIMO and mMISO cases using one reference per actuator achieved 6.1 dB_A and 2.0 dB_A attenuation, respectively over 315-400 Hz at the error arrays. Although performance was degraded by 4 dB_A, the number of computations required by mMISO was 512 times less. Using mMISO with two references per actuator increased performance to 2.7 dB_A and still required a factor of 256 fewer computations than the MIMO case using only one reference per actuator.

It should also be noted that fully coupled MIMO control using either two or three references per channel achieved 7.5 dB_A attenuation within the 315-400 Hz control band at the error microphones. However sound levels at observer microphones increased for all these cases by as much as 2 dB_A. Reasons for this are unknown at this stage and require further investigation.

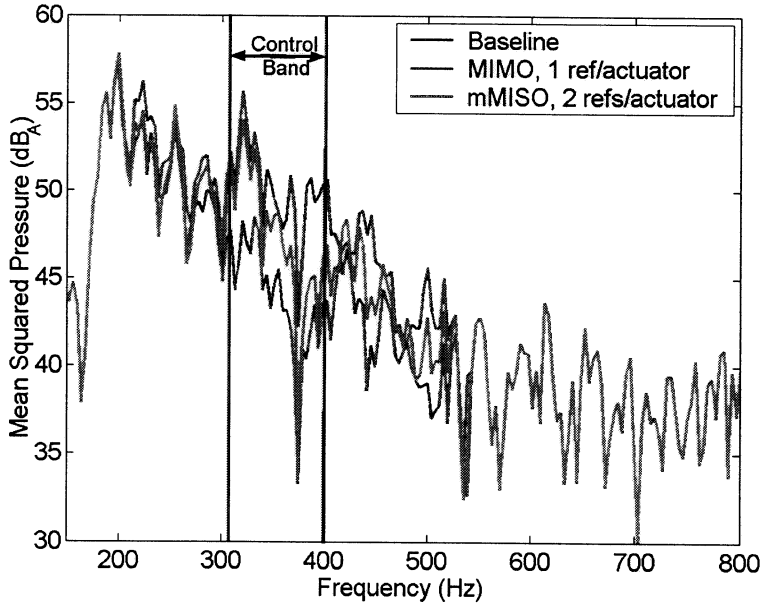

Figure 17. Comparison Between MIMO and mMISO Control with near field sensors.

[1] Note that mSISO control is mMISO control with a single reference per actuator.

B4. Summary

Several new important findings were determined by this research effort. In particular, the use of multiple references per actuator results in greater multiple coherence between structure vibration and the interior noise field and thus improved performance

A multiple uncoupled SISO controller system was developed and tested. Compared to MIMO control using a singular reference per actuator, mMISO performance was comparable. In addition it has the added benefit of significantly reducing the DSP computational overhead.

Error arrays were designed to reject near field acoustics. Their design allowed error sensors to be placed closer to the radiating panel while still achieving control at the error sensors. In addition, the error arrays were designed to be directional within the bandwidth of desired control such that they would physically decouple the system allowing mSISO/mMISO control to be more effective. Although good attenuation was achieved at the error sensors this was not reflected at the far field microphones whose levels slightly increased with control. Likely reasons are lack of near field resolution, non anechoic behavior of the enclosure or flanking path transmission through the enclosure. This behavior needs further investigation.

The work has successfully further developed the smart foam system towards more practical realizations.

C. References:

1. C. R. Fuller, Maillard, J.P., M. Mercadal, and A. H. von Flotow, "Control of aircraft interior noise using globally detuned vibration absorbers," *Proceedings of First Joint CEAS/AIAA Aeroacoustics Conference,* 1995.

2. J. A. Nelder and R. Mead, "A simplex method for function minimization," *The Computer Journal,* 7:308-313, 1965.

PERSONNEL SUPPORTED

Prof. Chris R. Fuller, PI
Dr. Mike Kidner, Research Associate
Mr. John D'Angelo, Graduate Student
Mr. Rick Wright, Graduate Student

PUBLICATIONS

Keynote Presentations

Fuller, C. R., "Energy Methods In Active Noise and Vibration Control", *Keynote Address,* NOVEM 2000 International Conference, Lyon, France, August 31-September 2, 2000.

Books or book chapters

Fuller, C. R., "Smart Skins for Sound Control," Volume 2, pp. 1029-1037, *The Encyclopedia of Smart Materials*, John Wiley and Sons, Inc., October, 2001.

C. R. Fuller, "Active Control: Feedforward Control of Vibration," Volume 2, pp. 513-520, *The Encyclopedia of Vibrations*, S. G. Braun, D. J. Ewins and S. S. Rao, Editor, Academic Press, September, 2001.

Journal Papers

Cabell, R. H. and Fuller, C. R., "A Principal Component Algorithm for Feedforward Active Noise and Vibration Control," *Journal of Sound and Vibration,* 227(1), pp. 159-181, 1999.

Guigou, C. and Fuller, C. R., "Control of Aircraft Interior Broadband Noise with Foam-PVDF Smart Skin," *Journal of Sound and Vibration*, 220(3), pp. 541-557, February, 1999.

Invited Papers

Fuller, C. R., "Smart Materials, Active-Passive Hybrid Noise Control Systems," Invited Presentation at the SEA Tech-Club, Troy, MI, March 8, 2001.

Conference Papers

Mathur, G. P., Fuller, C. R., Kidner, M. and P. Marcotte, "Aircraft Cabin Noise Control with Smart Foam Treatment on Fuselage Sidewall – Laboratory Tests," AIAA-2001-2231, Holland, May, 2001.

Fuller, C. R., Johnson, M. and Griffin, J., "Active-Passive Control of Interior Boundary Layer Noise Using Smart Foam," AIAA-2000-2041, 6th AIAA/CEAS Aeroacoustics Conference, Lahaina, Hawaii, June 12-14, 2000.

Presentations

Mathur, G., Fuller, C. R., Johnson, M. E. and D' Angelo, J., "Laboratory Testing of Smart Foam Lined Aircraft Trim Panels," Presentation at the 4th AST Interior Noise Workshop, Hampton, VA, February 15-17, 2000.

Fuller, C. R., D' Angelo, J., Johnson, M. E. and Griffin, J., "Control of Interior Noise Using Smart Foam Systems," Presentation at the 4th AST Interior Noise Workshop, Hampton, VA, February 15-17, 2000.

Wright, R., Fuller, C. R. and Johnson, M. E., "Control of Interior Noise Using Adaptive Tuned Vibration Absorbers," Presentation at the 4th AST Interior Noise Workshop, Hampton, VA, February 15-17, 2000.

Submitted papers

Carneal, J. and Fuller, C. R., "An Analytical Investigation of Active Structural Acoustic Control of Noise Transmission Through Double Panel Systems," submitted to *JSV*, 2002.

Carneal, J., Charette, F. and Fuller, C. R., "Minimization of Sound Radiation from Plates Using Adaptive Tuned Vibration Absorbers," submitted to *JASA*, 2002.

ACKNOWLEDGEMENTS

The VAL Va Tech research team gratefully acknowledges extremely useful technical interactions, support and suggestions from Dan Palumbo (Grant Technical Monitor), Rich Silcox, Gary Gibbs and Ran Cabell of the Structural Acoustics Branch at NASA Langley Research Center.